VQGRAPH: RETHINKING GRAPH REPRESENTATION SPACE FOR BRIDGING GNNS AND MLPS

Ling Yang[1] **Ye Tian**[1*] **Minkai Xu**[3] **Zhongyi Liu**[2] **Shenda Hong**[1] **Wei Qu**[2]
Wentao Zhang[1] **Bin Cui**[1†] **Muhan Zhang**[1†] **Jure Leskovec**[3]
[1]Peking University [2]Ant Group [3]Stanford University
yangling0818@163.com, tyfeld@stu.pku.edu.cn,
{zhongyi.lzy, qingze.qw}@antgroup.com, {minkai, jure}@cs.stanford.edu
{hongshenda, wentao.zhang, bin.cui, muhan}@pku.edu.cn

ABSTRACT

GNN-to-MLP distillation aims to utilize knowledge distillation (KD) to learn computationally-efficient multi-layer perceptron (student MLP) on graph data by mimicking the output representations of teacher GNN. Existing methods mainly make the MLP to mimic the GNN predictions over a few class labels. However, the class space may not be expressive enough for covering numerous diverse local graph structures, thus limiting the performance of knowledge transfer from GNN to MLP. To address this issue, we propose to learn a new powerful graph representation space by directly labeling nodes' diverse local structures for GNN-to-MLP distillation. Specifically, we propose a variant of VQ-VAE (Van Den Oord et al., 2017) to learn a structure-aware tokenizer on graph data that can encode each node's local substructure as a discrete code. The discrete codes constitute a *codebook* as a new graph representation space that is able to identify different local graph structures of nodes with the corresponding code indices. Then, based on the learned codebook, we propose a new distillation target, namely *soft code assignments*, to directly transfer the structural knowledge of each node from GNN to MLP. The resulting framework VQGRAPH achieves new state-of-the-art performance on GNN-to-MLP distillation in both transductive and inductive settings across seven graph datasets. We show that VQGRAPH with better performance infers faster than GNNs by 828×, and also achieves accuracy improvement over GNNs and stand-alone MLPs by 3.90% and 28.05% on average, respectively. Our code is available at https://github.com/YangLing0818/VQGraph

1 INTRODUCTION

Graph Neural Networks (GNNs) (Yang & Hong, 2022; Li et al., 2020a; Perozzi et al., 2014; Xu et al., 2019; Morris et al., 2019; Li et al., 2019; Chen et al., 2020b) have been widely used due to their effectiveness in dealing with non-Euclidean structured data, and have achieved remarkable performances in various graph-related tasks (Hamilton et al., 2017; Kipf & Welling, 2017; Veličković et al., 2018). Modern GNNs rely on message passing mechanism to learn node representations (Wu et al., 2020; Zhou et al., 2020). GNNs have been especially important for recommender systems (Fan et al., 2019; He et al., 2020; Guo et al., 2020; Wu et al., 2022), fraud detection (Dou et al., 2020; Liu et al., 2021), and information retrieval (Li et al., 2020b; Mao et al., 2020). Numerous works (Pei et al., 2020b) focus on exploring more effective ways to leverage informative neighborhood structure for improving GNNs (Park et al., 2021; Zhu et al., 2021; Zhao et al., 2022; Tang et al., 2022; Lee et al., 2021; Chien et al., 2022; Abu-El-Haija et al., 2019).

It is challenging to scale GNNs to large-scale applications which are constrained by latency and require fast inference (Zhang et al., 2020; 2022a; Jia et al., 2020), because message passing necessitates fetching topology and features of many neighbor nodes for inference on a target node, which

[*]Contributed equally.
[†]Corresponding authors.

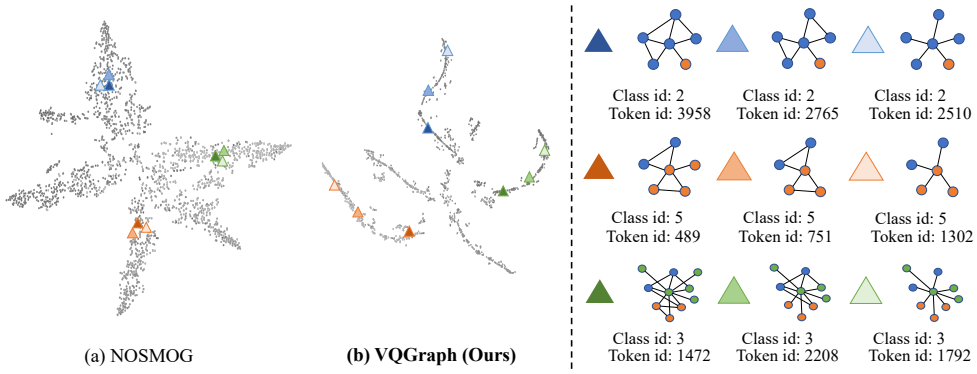

(a) NOSMOG **(b) VQGraph (Ours)**

Figure 1: The t-SNE visualization of the learned graph representation space in two kinds of teacher GNNs: (a) previous SOTA "class-based" NOSMOG (Tian et al., 2023b) and (b) our "structure-based" VQGraph. "class-based" denotes learning with class labels, and "structure-based" denotes learning with our local structure reconstruction. Our learned space is more compact. We here provide both class labels and our structure labels along with illustrative substructures for demonstration.

is time-consuming and computation-intensive. Multi-layer perceptrons (MLPs) are efficient alternatives to deploy on graphs that only depend on node feature without the need of explicit message passing (Zhang et al., 2022b). Thus, recent methods use *knowledge distillation* (Hinton et al., 2015; Tian et al., 2023a; Gou et al., 2021; Yuan et al., 2020; Zhou & Song, 2021) to transfer the learned structural knowledge from GNNs to MLPs (Zhang et al., 2022b; Zheng et al., 2022; Tian et al., 2023b), which build the statistical associations between node features and class labels by making the MLP mimic the (well-trained) GNN's predictions. Then only MLPs are deployed for inference, which can also perform well in real-world graphs.

Despite some progress, current GNN-to-MLP distillation methods have a common fundamental issue: their graph representation spaces of GNN are mainly learned by a few class labels, and the class space may not be expressive enough for covering numerous diverse local graph structures of nodes, limiting the distillation performance. We explain this problem by using t-SNE (Van der Maaten & Hinton, 2008) to visualize the graph representation space as in Figure 1. We can observe that the graph representation space in previous teacher GNN is not expressive enough for identifying fine-grained local structural differences between nodes of the same class, which may limit the structural knowledge transfer from GNN to MLP.

Here we introduce a new powerful graph representation space for bridging GNNs and MLPs by directly labeling diverse nodes' local structures. Specifically, we propose a variant of VQ-VAE (Van Den Oord et al., 2017) to learn a structure-aware tokenizer on graph data that can encode each node with its substructure as a discrete code. The numerous codes constitute a *codebook* as our new graph representation space that is able to identify different local neighborhood structures of nodes with the corresponding code indices. As demonstrated in Figure 1, our learned representation space is more expressive and can identify subtle differences between nodes' local structures. Based on the learned codebook, we can effectively facilitate the structure-based distillation by maximizing the consistency of *soft code assignments* between GNN and MLP models, given by the KL divergence between GNN predictions and MLP predictions over the discrete codes of the codebook.

We highlight our main contributions as follows: **(i)** To the best of our knowledge, we for the first time directly learn to label nodes' local neighborhood structures to acquire a powerful node representation space (*i.e.*, a *codebook*) for bridging GNNs and MLPs. **(ii)** Based on the learned codebook, we utlize a new distillation target with *soft code assignments* to effectively facilitate the structure-aware knowledge distillation. We further conduct both visualization and statistical analyses for better understanding with respect to our superior local and global structure awareness for GNN-to-MLP distillation. **(iii)** Extensive experiments across seven datasets show VQGraph can consistently outperform GNNs by **3.90%** on average accuracy, while enjoying **828×** faster inference speed. Also VQGraph outperforms MLPs and SOTA distillation method NOSMOG (Tian et al., 2023b) by **28.05% and 1.39%** on average accuracy across datasets, respectively.

2 Related Work

Inference Acceleration for GNNs Pruning (Zhou et al., 2021) and quantizing GNN parameters (Zhao et al., 2020) have been studied for inference acceleration (Chen et al., 2016; Judd et al.,

2016; Han et al., 2015; Gupta et al., 2015). Although these approaches accelerate GNN inference to a certain extent, they do not eliminate the neighbor-fetching latency. Graph-MLP (Hu et al., 2021) proposes to bypass GNN neighbor fetching by learning a computationally-efficient MLP model with a neighbor contrastive loss, but its paradigm is only transductive and can be not applied in the more practical inductive setting. Besides, some works try to speed up GNN in training stage from the perspective of node sampling (Zou et al., 2019; Chen et al., 2018c), which are complementary to our goal on inference acceleration.

Knowledge Distillation for GNNs Existing GNN-based knowledge distillation methods try to distill teacher GNNs to smaller student GNNs (GNN-GNN distillation) or MLPs (GNN-to-MLP distillation). Regarding the GNN-GNN distillation, LSP (Yang et al., 2021c), TinyGNN (Yan et al., 2020), GFKD (Deng & Zhang, 2021), and GraphSAIL (Xu et al., 2020) conduct KD by enabling student GNN to maximally preserve local information that exists in teacher GNN. The student in CPF (Yang et al., 2021b) is not a GNN, but it is still heavily graph-dependent as it uses LP (Zhu & Ghahramanih, 2002; Huang et al., 2021). Thus, these methods still require time-consuming neighbors fetching. To address these latency issues, recent works focus on GNN-to-MLP distillation that does not require message passing, as seen in (Hu et al., 2021; Zhang et al., 2022b; Zheng et al., 2022; Tian et al., 2023b). For example, recent sota methods GLNN (Zhang et al., 2022b) and NOSMOG (Tian et al., 2023b) train the student MLP with node features as inputs and class predictions from the teacher GNN as targets. However, class predictions over a few labels, as their distillation targets, can not sufficiently express structural knowledge of graph structures as discussed in Sec. 1. Hence, we for the first time propose to directly label nodes' local neighborhood structures to facilitate structure-aware knowledge distillation.

3 PRELIMINARIES

Notation and Graph Neural Networks We denote a graph as $\mathcal{G} = (\mathcal{V}, \boldsymbol{A})$, with $\mathcal{V} = \{\boldsymbol{v}_1, \boldsymbol{v}_2, \cdots, \boldsymbol{v}_n\}$ represents all nodes, and $\boldsymbol{A}$ denotes adjacency matrix, with $A_{i,j} = 1$ if node $\boldsymbol{v}_i$ and node $\boldsymbol{v}_j$ are connected, and 0 otherwise. Let N denote the total number of nodes. $\boldsymbol{X} \in \mathbb{R}^{N \times D}$ represents the node feature matrix with each raw being a D-dimensional node attribute $\boldsymbol{v}$. For node classification, the prediction targets are $\boldsymbol{Y} \in \mathbb{R}^{N \times K}$, where row $\boldsymbol{y}_v$ is a K-dim one-hot vector for node v. For a given $\mathcal{G}$, usually a small portion of nodes will be labeled, which we mark using superscript ^{L}, i.e. $\mathcal{V}^L$, $\boldsymbol{X}^L$ and $\boldsymbol{Y}^L$. The majority of nodes will be unlabeled, and we mark using the superscript ^{U}, i.e. $\mathcal{V}^U$, $\boldsymbol{Y}^U$ and $\boldsymbol{Y}^U$. For a given node $\boldsymbol{v} \in \mathcal{V}$, GNNs aggregate the messages from node neighbors $\mathcal{N}(\boldsymbol{v})$ to learn node embedding $\boldsymbol{h}_{\boldsymbol{v}} \in \mathbb{R}^{d_n}$ with dimension d_n. Specifically, the node embedding in l-th layer $\boldsymbol{h}_{\boldsymbol{v}}^{(l)}$ is learned by first aggregating (AGG) the neighbor embeddings and then updating (UPDATE) it with the embedding from the previous layer. The whole learning process can be denoted as: $\boldsymbol{h}_{\boldsymbol{v}}^{(l)} = \text{UPDATE}(\boldsymbol{h}_{\boldsymbol{v}}^{(l-1)}, \text{AGG}(\{\boldsymbol{h}_{\boldsymbol{u}}^{(l-1)} : \boldsymbol{u} \in \mathcal{N}(\boldsymbol{v})\}))$.

Vector Quantized-Variational AutoEncoder (VQ-VAE) for Continuous Data The VQ-VAE model (Van Den Oord et al., 2017) is originally proposed for modeling continuous data distribution, such as images, audio and video. It encodes observations into a sequence of discrete latent variables, and reconstructs the observations from these discrete variables. Both encoder and decoder use a shared codebook. More formally, the encoder is a non-linear mapping from the input space, $\boldsymbol{x}$, to a vector $E(\boldsymbol{x})$. This vector is then quantized based on its distance to the prototype vectors (tokens) in the codebook $\boldsymbol{e}_k, k \in 1 \ldots K$ such that each vector $E(\boldsymbol{x})$ is replaced by the index of the nearest code in the codebook, and is transmitted to the decoder: $\text{quantize}(E(\mathbf{x})) = \mathbf{e}_k$, where $k = \arg\min_j ||E(\mathbf{x}) - \mathbf{e}_j||$. To learn these mappings, the gradient of the reconstruction error is then back-propagated through the decoder, and to the encoder using the straight-through gradient estimator (Bengio et al., 2013). Besides reconstruction loss, VQ-VAE has two additional terms to align the token space of the codebook with the output of the encoder. The *codebook loss*, which only applies to the codebook variables, brings the selected code $\mathbf{e}$ close to the output of the encoder, $E(\mathbf{x})$. The *commitment loss*, which only applies to the encoder weights, encourages the output of the encoder to stay close to the chosen code to prevent it from fluctuating too frequently from one code vector to another. The overall objective is:

$$\mathcal{L}(\mathbf{x}, D(\mathbf{e})) = ||\mathbf{x} - D(\mathbf{e})||_2^2 + ||\text{sg}[E(\mathbf{x})] - \mathbf{e}||_2^2 + \eta||\text{sg}[\mathbf{e}] - E(\mathbf{x})||_2^2, \tag{1}$$

where E is the encoder function and D is the decoder function. The operator sg refers to a stop-

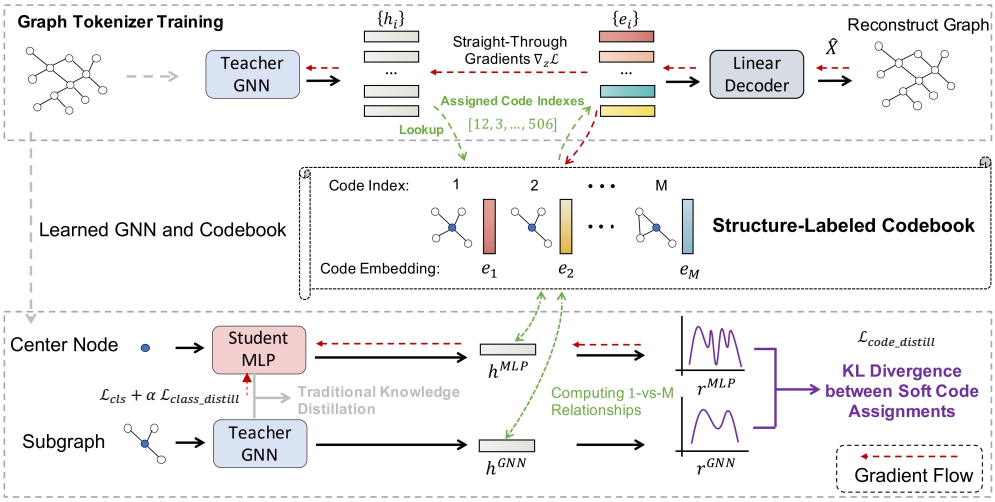

Figure 2: The schematic diagram of VQGRAPH, including graph tokenizer training (**Top**) and structure-aware code-based GNN-to-MLP Distillation (**Bottom**).

gradient operation that blocks gradients from flowing into its argument, and η is a hyperparameter which controls the reluctance to change the code corresponding to the encoder output. In this paper, **we explore the potential of VQ-VAE for representing discrete graph-structured data**.

4 VQGRAPH

The critical insights of VQGRAPH is learning an expressive graph representation space that directly labels nodes' diverse local neighborhood structures with different code indices for facilitating effective structure-aware GNN-to-MLP distillation. First, we learn a structure-aware graph tokenizer to encode the nodes with diverse local structures to corresponding discrete codes, and constitute a *codebook* (Sec. 4.1). Then we utilize the learned codebook for GNN-to-MLP distillation, and propose a tailored structure-aware distillation objective based on *soft code assignmnets* (Sec. 4.2).

4.1 GRAPH TOKENIZER TRAINING

Labeling Nodes' Local Structure with Discrete Codes Similar to the tokenization in NLP (Sennrich et al., 2016; Wu et al., 2016), we tokenize the nodes with different neighborhood structures as discrete codes using a variant of VQ-VAE (Van Den Oord et al., 2017), *i.e.*, a graph tokenizer that consists of a GNN encoder and a codebook. More concretely, the nodes $\mathcal{V} = \{\boldsymbol{v}_1, \boldsymbol{v}_2, \cdots, \boldsymbol{v}_n\}$ of a graph $\mathcal{G}$ are tokenized to $\mathcal{Z} = \{z_1, z_2, \cdots, z_n\}$, where the codebook contains M discrete codes. Firstly, the teacher GNN encoder encodes the nodes to nodes embeddings. Next, our graph tokenizer looks up the nearest neighbor code embedding in the codebook for each node embedding $\boldsymbol{h}_i$. Let $\boldsymbol{E} = [\boldsymbol{e}_1, \boldsymbol{e}_2, \cdots, \boldsymbol{e}_M] \in \mathbb{R}^{M \times D}$ denote the codebook embeddings, which are randomly initialized and are then optimized in pretraining. The assigned code of i-th node is:

$$z_i = \text{argmin}_j \|\boldsymbol{h}_i - \boldsymbol{e}_j\|_2, \tag{2}$$

We feed the corresponding codebook embeddings $\{\boldsymbol{e}_{z_1}, \boldsymbol{e}_{z_2}, \cdots, \boldsymbol{e}_{z_n}\}$ to the linear decoder ($p_\psi : \boldsymbol{e}_{z_i} \to \hat{\boldsymbol{v}}_i$) to reconstruct the input graph including both nodes attributes $\boldsymbol{X} \in \mathbb{R}^{N \times D}$ and adjacency matrix $\boldsymbol{A} \in \mathbb{R}^{N \times N}$ for an end-to-end optimization of our graph tokenizer.

Graph Tokenizer Optimization We adapt VQ-VAE (first term in Equation (1)) to fit our graph tokenization. In addition, the categorical information is also critical for node representations, thus we integrate it into the optimization of our graph tokenizer:

$$\mathcal{L}_{Rec} = \underbrace{\frac{1}{N}\sum_{i=1}^{N}\left(1 - \frac{\boldsymbol{v}_i{}^T \hat{\boldsymbol{v}}_i}{\|\boldsymbol{v}_i\| \cdot \|\hat{\boldsymbol{v}}_i\|}\right)^\gamma}_{\text{node reconstruction}} + \underbrace{\left\|\boldsymbol{A} - \sigma(\hat{\boldsymbol{X}} \cdot \hat{\boldsymbol{X}}^T)\right\|_2^2}_{\text{edge reconstruction}}, \tag{3}$$

$$\mathcal{L}_{Tokenizer} = \mathcal{L}_{Rec} + \mathcal{L}_{CE}(\boldsymbol{y}_{\{\boldsymbol{v}_i\}}, \hat{\boldsymbol{y}}_{\{\boldsymbol{e}_{z_i}\}}) + \frac{1}{N}\sum_{i=1}^{N}\|\text{sg}[\boldsymbol{h}_i] - \boldsymbol{e}_{z_i}\|_2^2 + \frac{\eta}{N}\sum_{i=1}^{N}\|\text{sg}[\boldsymbol{e}_{z_i}] - \boldsymbol{h}_i\|_2^2,$$

where $\hat{\boldsymbol{v}} \in \mathbb{R}^D$ and $\hat{\boldsymbol{X}} \in \mathbb{R}^{N \times D}$ denote the predicted node embedding and node embedding matrix, respectively. sg$[\cdot]$ stands for the stopgradient operator, and the flow of gradients is illustrated in Figure 2. $\mathcal{L}_{Rec}$ denotes the graph reconstruction loss, aiming to preserve node attributes by the first node reconstruction term with the scaled cosine error ($\gamma \geq 1$), and recover graph structures by the second topology reconstruction term. $\mathcal{L}_{CE}$ is the cross-entropy loss between labels $\boldsymbol{y}_{\{\boldsymbol{v}_i\}}$ and the GNN predictions $\hat{\boldsymbol{y}}_{\{\boldsymbol{e}_{z_i}\}}$ that are based on the assigned codes $\{\boldsymbol{e}_{z_i}\}$. In $\mathcal{L}_{Tokenizer}$, the third term is a VQ loss aiming to update the codebook embeddings and the forth term is a commitment loss that encourages the output of the GNN encoder to stay close to the chosen code embedding. η is a hyper-parameter set to 0.25 in our experiments. With the learned graph tokenizer, we acquire a powerful codebook that not only directly identifies local graph structures, but also preserves class information for node representations, facilitating later GNN-to-MLP distillation.

Clarifying Superiority over VQ-VAE and Graph AutoEncoders In contrast to vanilla VQ-VAE, we provide a new variant of VQ-VAE for modeling discrete graph data instead of continuous data, and utilize the learned codebook for distillation task instead of generation tasks. In contrast to traditional graph autoencoders (Kipf & Welling, 2016), our model does not suffer from large variance (Van Den Oord et al., 2017). And with our expressive latent codes, we can effectively avoid "posterior collapse" issue which has been problematic with many graph AE models that have a powerful decoder, often caused by latents being ignored. We provide experimental comparison to demonstrate our superiority in Sec. 5.3.

Scaling to Large-Scale Graphs We have introduced the main pipeline of graph tokenizer training based on the entire graph input. Nevertheless, for large-scale industrial applications, one can not feed the whole graph due to the latency constraint (Fey et al., 2021; Bojchevski et al., 2020; Ying et al., 2018; Chen et al., 2020a). Numerous researches choose subgraph-wise sampling methods as a promising class of mini-batch training techniques (Chen et al., 2018b;a; Zeng et al., 2020; Huang et al., 2018; Chiang et al., 2019; Zou et al., 2019; Shi et al., 2023), implicitly covering the global context of graph structure through a number of stochastic re-sampling. We follow this technique to perform large-scale graph tokenizer training. For example, we adopt GraphSAGE (Hamilton et al., 2017) as teacher GNN, we samples the target nodes as a mini-batch $\mathcal{V}_{sample}$ and samples a fixed size set of neighbors for feature aggregation. We utilize the connections between the target nodes as the topology reconstruction target (the second term of $\mathcal{L}_{Rec}$ in Equation (3)) for approximately learning global graph structural information.

4.2 Structure-Aware Code-Based GNN-to-MLP Distillation

After the graph tokenizer optimization, we obtain a pre-trained teacher GNN encoder and a set of codebook embeddings $\boldsymbol{E}$. We hope to distill the structure knowledge node-by-node from the GNN to a student MLP based on the codebook. Next, we will introduce our tailored structure-aware GNN-to-MLP distillation with the *soft code assignments* over the learned codebook.

Aligning Soft Code Assignments Between GNN and MLP Different from previous class-based distillation methods (Zhang et al., 2022b; Tian et al., 2023b) that constrain on class predictions between GNN and MLP, we utilize a more expressive representation space of graph data, *i.e.*, our structure-aware codebook, and propose code-based distillation to leverage more essential information of graph structures for bridging GNN and MLP. Formally, for each node $\boldsymbol{v}_i$, we have its GNN representation $\boldsymbol{h}_i^{\text{GNN}} \in \mathbb{R}^D$ and the MLP representation $\boldsymbol{h}_i^{\text{MLP}} \in \mathbb{R}^D$. Then we respectively compare their node representations with all M codes of the codebook embeddings $\boldsymbol{E} \in \mathbb{R}^{M \times D}$ and obtain corresponding *soft code assignments* $\boldsymbol{r}_i^{\text{GNN}} \in \mathbb{R}^M$ and $\boldsymbol{r}_i^{\text{MLP}} \in \mathbb{R}^M$:

$$\boldsymbol{r}_i^{\text{GNN}} = \text{COMP}(\boldsymbol{h}_i^{\text{GNN}}, \boldsymbol{E}), \quad \boldsymbol{r}_i^{\text{MLP}} = \text{COMP}(\boldsymbol{h}_i^{\text{MLP}}, \boldsymbol{E}), \tag{4}$$

where COMP : $[\mathbb{R}^D, \mathbb{R}^{M \times D}] \rightarrow \mathbb{R}^M$ can be arbitrary relation module for computing 1-*vs*-M code-wise relations, and such relations can be viewed as assignment possibilities. We use L_2 distance in our experiments (more studies in Appendix C.1). Kindly note that the codebook size M can be large, especially for large-scale graphs, thus the soft code assignment of each node contains abundant 1-*vs*-M global structure-discriminative information. Therefore we choose the soft code assignment as

the target for final distillation:

$$\mathcal{L}_{code_distill} = \frac{1}{N}\sum_{i=1}^{N} \tau^2 \, \mathrm{KL}(\boldsymbol{p}_i^{\mathrm{GNN}} \parallel \boldsymbol{p}_i^{\mathrm{MLP}}) = \frac{1}{N}\sum_{i=1}^{N} \tau^2 \, \boldsymbol{p}_i^{\mathrm{GNN}} \log \frac{\boldsymbol{p}_i^{\mathrm{GNN}}}{\boldsymbol{p}_i^{\mathrm{MLP}}}, \tag{5}$$

where KL refers to Kullback–Leibler divergence with:

$$\boldsymbol{p}_i^{\mathrm{GNN}} = \mathrm{Softmax}(\boldsymbol{r}_i^{\mathrm{GNN}}/\tau), \quad \boldsymbol{p}_i^{\mathrm{MLP}} = \mathrm{Softmax}(\boldsymbol{r}_i^{\mathrm{MLP}}/\tau), \tag{6}$$

being the scaled code assignments, and τ is the temperature factor to control the softness. Kindly note that the code assignment is only used for optimizing the training, and we remove it for deploying the pure MLP model. In this way, VQGRAPH is able to effectively distill both local neighborhood structural knowledge and global structure-discriminative ability from GNNs to MLPs, without increasing inference time. The overall training loss of VQGRAPH is composed of classification loss $\mathcal{L}_{cls}$, traditional class-based distillation loss $\mathcal{L}_{class_distill}$, and our code-based distillation loss, i.e.,

$$\mathcal{L}_{\mathrm{VQGRAPH}} = \mathcal{L}_{cls} + \alpha\mathcal{L}_{class_distill} + \beta\mathcal{L}_{code_distill}. \tag{7}$$

where α and β are factors for balancing the losses.

5 EXPERIMENTS

Datasets and Evaluation We use five widely used public benchmark datasets (Zhang et al., 2022b; Yang et al., 2021a) (`Citeseer`, `Pubmed`, `Cora`, `A-computer`, and `A-photo`), and two large OGB datasets (Hu et al., 2020a) (`Arxiv` and `Products`) to evaluate the proposed model. In our experiments, we report the mean and standard deviation of ten distinct runs with randomized seeds to ensure robustness and reliability of our findings. **We also extend our VQGRAPH to heterophilic graphs and make performance improvement in Appendix A.2**. We utilize accuracy to gauge model performance. More details are in Appendix B.1.

Model Architectures For fair comparison, we adopt GraphSAGE with GCN aggregation as our teacher model (also as graph tokenizer) and use the same student MLP models for all evaluations following SOTA GLNN (Zhang et al., 2022b) and NOSMOG (Tian et al., 2023b). The codebook size increases accordingly with dataset size (studied in Sec. 5.3). For example, we set 2048 and 8192 for `Cora` and `A-photo`, respectively. More model hyperparameters are detailed in Appendix B.2. We investigate the influence of alternative teacher models, including GCN (Kipf & Welling, 2017), GAT (Veličković et al., 2018), and APPNP (Klicpera et al., 2019), detailed in Appendix C.2.

Transductive vs. Inductive We experiment in two separate settings, transductive (*tran*) and inductive (*ind*), for comprehensive evaluation. In both settings, we first pre-train our graph tokenizer to learn the codebook embeddings $\boldsymbol{E}$ for code-based distillation. For the *tran* setting, we train our models on the labeled graph $\mathcal{G}$, along with the corresponding feature matrix $\boldsymbol{X}^L$ and label vector $\boldsymbol{Y}^L$, before evaluating their performance on the unlabeled data $\boldsymbol{X}^U$ and $\boldsymbol{Y}^U$. Soft labels, soft code assignments are generated for all nodes within the graph (i.e., $\boldsymbol{y}_{\boldsymbol{v}}^{soft}$, $\boldsymbol{r}_{\boldsymbol{v}}^{GNN}$, $\boldsymbol{r}_{\boldsymbol{v}}^{MLP}$ for $\boldsymbol{v} \in \mathcal{V}$). As for *ind*, we follow the methodology of prior work (Tian et al., 2023b) in randomly selecting 20% of the data for inductive evaluation. Specifically, we divide the unlabeled nodes $\mathcal{V}^U$ into two separate yet non-overlapping subsets, observed and inductive (i.e., $\mathcal{V}^U = \mathcal{V}_{obs}^U \sqcup \mathcal{V}_{ind}^U$), producing three distinct graphs, $\mathcal{G} = \mathcal{G}^L \sqcup \mathcal{G}_{obs}^U \sqcup \mathcal{G}_{ind}^U$, wherein there are no shared nodes. In training, the edges between $\mathcal{G}^L \sqcup \mathcal{G}_{obs}^U$ and $\mathcal{G}_{ind}^U$ are removed, while they are leveraged during inference to transfer positional features via average operator (Hamilton et al., 2017). Node features and labels are partitioned into three disjoint sets, *i.e.*, $\boldsymbol{X} = \boldsymbol{X}^L \sqcup \boldsymbol{X}_{obs}^U \sqcup \boldsymbol{X}_{ind}^U$ and $\boldsymbol{Y} = \boldsymbol{Y}^L \sqcup \boldsymbol{Y}_{obs}^U \sqcup \boldsymbol{Y}_{ind}^U$. Soft labels and soft code assignments are generated for nodes within the labeled and observed subsets (i.e., $\boldsymbol{y}_{\boldsymbol{v}}^{soft}$, $\boldsymbol{r}_{\boldsymbol{v}}^{GNN}$, $\boldsymbol{r}_{\boldsymbol{v}}^{MLP}$ for $\boldsymbol{v} \in \mathcal{V}^L \sqcup \mathcal{V}_{obs}^U$). We provide code and models in the supplementary material.

5.1 MAIN RESULTS

GNN-to-MLP Distillation We compare VQGRAPH to other state-of-the-art GNN-to-MLP distillation methods GLNN and NOSMOG with same experimental settings, and use distilled MLP models for evaluations. We first consider the standard transductive setting, enabling direct comparison with previously published literature (Zhang et al., 2022b; Hu et al., 2020b; Yang et al., 2021a). As depicted in Tab. 1, VQGRAPH outperforms all baselines including teacher GNN models across

Table 1: Node classification results under the standard setting, results show accuracy (higher is better). Δ_{GNN}, Δ_{MLP}, Δ_{NOSMOG} represents the difference between VQGRAPH and GNN, MLP, NOSMOG, respectively. GLNN and NOSMOG are the SOTA GNN-to-MLP distillation methods.

Datasets	SAGE	MLP	GLNN	NOSMOG	**VQGRAPH**	Δ_{GNN}	Δ_{MLP}	Δ_{NOSMOG}
Citeseer	70.49 ± 1.53	58.50 ± 1.86	71.22 ± 1.50	73.78 ± 1.54	$\mathbf{76.08 \pm 0.55}$	$\uparrow 7.93\%$	$\uparrow 30.05\%$	$\uparrow 3.18\%$
Pubmed	75.56 ± 2.06	68.39 ± 3.09	75.59 ± 2.46	77.34 ± 2.36	$\mathbf{78.40 \pm 1.71}$	$\uparrow 3.76\%$	$\uparrow 14.64\%$	$\uparrow 1.37\%$
Cora	80.64 ± 1.57	59.18 ± 1.60	80.26 ± 1.66	83.04 ± 1.26	$\mathbf{83.93 \pm 0.87}$	$\uparrow 4.08\%$	$\uparrow 41.82\%$	$\uparrow 1.07\%$
A-computer	82.82 ± 1.37	67.62 ± 2.21	82.71 ± 1.18	84.04 ± 1.01	$\mathbf{85.17 \pm 1.29}$	$\uparrow 2.84\%$	$\uparrow 25.95\%$	$\uparrow 1.34\%$
A-photo	90.85 ± 0.87	77.29 ± 1.79	91.95 ± 1.04	93.36 ± 0.69	$\mathbf{94.21 \pm 0.45}$	$\uparrow 3.70\%$	$\uparrow 21.89\%$	$\uparrow 0.91\%$
Arxiv	70.73 ± 0.35	55.67 ± 0.24	63.75 ± 0.48	71.65 ± 0.29	$\mathbf{72.43 \pm 0.20}$	$\uparrow 2.40\%$	$\uparrow 30.11\%$	$\uparrow 0.93\%$
Products	77.17 ± 0.32	60.02 ± 0.10	63.71 ± 0.31	78.45 ± 0.38	$\mathbf{79.17 \pm 0.21}$	$\uparrow 2.59\%$	$\uparrow 31.91\%$	$\uparrow 0.92\%$

Table 2: Node classification results in a production scenario with both **inductive** and **transductive** settings. *ind* indicates the results on $\mathcal{V}_{ind}^{U}$, *tran* indicates the results on $\mathcal{V}_{tran}^{U}$, and *prod* indicates the interpolated production results of both ind and $tran$.

Datasets	Eval	SAGE	MLP	GLNN	NOSMOG	**VQGRAPH**	Δ_{GNN}	Δ_{MLP}	Δ_{NOSMOG}
Citeseer	*prod*	68.06	58.49	69.08	70.60	**73.76**	$\uparrow 8.37\%$	$\uparrow 26.11\%$	$\uparrow 5.80\%$
	ind	69.14 ± 2.99	59.31 ± 4.56	68.48 ± 2.38	70.30 ± 2.30	$\mathbf{72.93 \pm 1.78}$	$\uparrow 5.48\%$	$\uparrow 22.96\%$	$\uparrow 3.74\%$
	tran	67.79 ± 2.80	58.29 ± 1.94	69.23 ± 2.39	70.67 ± 2.25	$\mathbf{74.59 \pm 1.94}$	$\uparrow 10.03\%$	$\uparrow 27.96\%$	$\uparrow 7.74\%$
Pubmed	*prod*	74.77	68.39	74.67	75.82	**76.92**	$\uparrow 2.86\%$	$\uparrow 12.47\%$	$\uparrow 1.45\%$
	ind	75.07 ± 2.89	68.28 ± 3.25	74.52 ± 2.95	75.87 ± 3.32	$\mathbf{76.71 \pm 2.76}$	$\uparrow 2.18\%$	$\uparrow 12.35\%$	$\uparrow 1.11\%$
	tran	74.70 ± 2.33	68.42 ± 3.06	74.70 ± 2.75	75.80 ± 3.06	$\mathbf{77.13 \pm 3.01}$	$\uparrow 3.25\%$	$\uparrow 12.73\%$	$\uparrow 1.75\%$
Cora	*prod*	79.53	59.18	77.82	81.02	**81.68**	$\uparrow 2.70\%$	$\uparrow 38.02\%$	$\uparrow 0.81\%$
	ind	81.03 ± 1.71	59.44 ± 3.36	73.21 ± 1.50	81.36 ± 1.53	$\mathbf{82.20 \pm 1.32}$	$\uparrow 1.44\%$	$\uparrow 38.29\%$	$\uparrow 1.03\%$
	tran	79.16 ± 1.60	59.12 ± 1.49	78.97 ± 1.56	80.93 ± 1.65	$\mathbf{81.15 \pm 1.25}$	$\uparrow 2.51\%$	$\uparrow 37.26\%$	$\uparrow 0.27\%$
A-computer	*prod*	82.73	67.62	82.10	83.85	**84.16**	$\uparrow 1.73\%$	$\uparrow 24.46\%$	$\uparrow 0.37\%$
	ind	82.83 ± 1.51	67.69 ± 2.20	80.27 ± 2.11	84.36 ± 1.57	$\mathbf{85.73 \pm 2.04}$	$\uparrow 3.50\%$	$\uparrow 26.65\%$	$\uparrow 1.62\%$
	tran	82.70 ± 1.34	67.60 ± 2.23	82.56 ± 1.80	83.72 ± 1.44	$\mathbf{84.56 \pm 1.81}$	$\uparrow 2.25\%$	$\uparrow 25.08\%$	$\uparrow 1.00\%$
A-photo	*prod*	90.45	77.29	91.34	92.47	**93.05**	$\uparrow 2.87\%$	$\uparrow 20.39\%$	$\uparrow 0.62\%$
	ind	90.56 ± 1.47	77.44 ± 1.50	89.50 ± 1.12	92.61 ± 1.09	$\mathbf{93.11 \pm 0.89}$	$\uparrow 2.82\%$	$\uparrow 20.24\%$	$\uparrow 0.54\%$
	tran	90.42 ± 0.68	77.25 ± 1.90	91.80 ± 0.49	92.44 ± 0.51	$\mathbf{92.96 \pm 1.02}$	$\uparrow 2.81\%$	$\uparrow 20.34\%$	$\uparrow 0.56\%$
Arxiv	*prod*	70.69	55.35	63.50	70.90	**71.43**	$\uparrow 1.05\%$	$\uparrow 29.05\%$	$\uparrow 0.75\%$
	ind	70.69 ± 0.58	55.29 ± 0.63	59.04 ± 0.46	70.09 ± 0.55	$\mathbf{70.86 \pm 0.42}$	$\uparrow 0.24\%$	$\uparrow 28.16\%$	$\uparrow 1.10\%$
	tran	70.69 ± 0.39	55.36 ± 0.34	64.61 ± 0.15	71.10 ± 0.34	$\mathbf{72.03 \pm 0.56}$	$\uparrow 1.90\%$	$\uparrow 30.11\%$	$\uparrow 1.31\%$
Products	*prod*	76.93	60.02	63.47	77.33	**77.93**	$\uparrow 1.30\%$	$\uparrow 29.84\%$	$\uparrow 0.77\%$
	ind	77.23 ± 0.24	60.02 ± 0.09	63.38 ± 0.33	77.02 ± 0.19	$\mathbf{77.50 \pm 0.25}$	$\uparrow 0.35\%$	$\uparrow 29.12\%$	$\uparrow 0.62\%$
	tran	76.86 ± 0.27	60.02 ± 0.11	63.49 ± 0.31	77.41 ± 0.21	$\mathbf{78.36 \pm 0.13}$	$\uparrow 1.95\%$	$\uparrow 30.56\%$	$\uparrow 1.23\%$

all datasets. Specifically, VQGRAPH improves performance **by an average of 3.90% compared to its teacher GNN**, highlighting its ability to capture superior structural information without relying on explicit graph structure input. Comparing VQGRAPH to NOSMOG, our proposed model **achieves an average improvement of 1.39%** across both small- and large-scale graph datasets. Further model analysis of VQGRAPH is presented in Sec. 5.3.

Experiments in Inductive and Transductive Settings To gain deeper insights into the effectiveness of VQGRAPH, we conduct experiments in a realistic production ($prod$) scenario that involves both inductive (ind) and transductive ($tran$) settings across multiple datasets, as detailed in Tab. 2. Our experimental results demonstrate that VQGRAPH consistently achieves superior performance compared to the teacher model and baseline methods across all datasets and settings. Specifically, our proposed method outperforms GNN across all datasets and settings with **an average improvement of 2.93%**, demonstrating its superior efficacy of our learned code-based representation space in capturing graph structural information, even on large-scale datasets. Furthermore, when compared to MLP and NOSMOG, VQGRAPH consistently achieves significant performance improvements, **with average gains of 25.81% and 1.6%**, respectively, across all datasets and settings.

5.2 MODEL ANALYSIS

Trade-off between Performance and Inference Time To demonstrate its efficiency and capacity of our VQGRAPH, we visualize the trade-off between node classification accuracy and model inference time on Citeseer dataset in Figure 3. Our results indicate that achieves a highest accuracy of 76% while maintaining a fast inference time of 1.45ms. Compared to the other models with similar inference time, VQGRAPH significantly **outperforms NOSMOG and MLPs by 3.12% and 30.05% in average accuracy**, respectively. For those models having comparable performance with VQGRAPH, they require a considerable amount of inference time, e.g., 2 layers GraphSAGE (SAGE-L2) needs 152.31ms and 3 layers GraphSAGE (SAGE-L3) needs 1201.28ms, making them

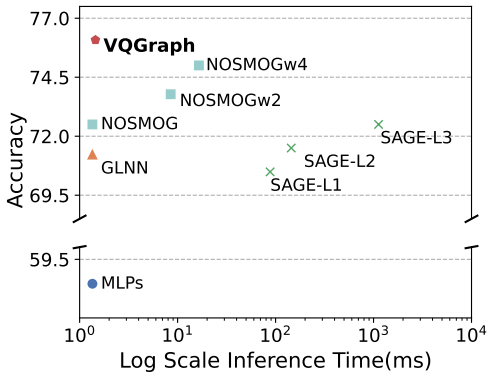

Figure 3: Accuracy vs. Inference Time.

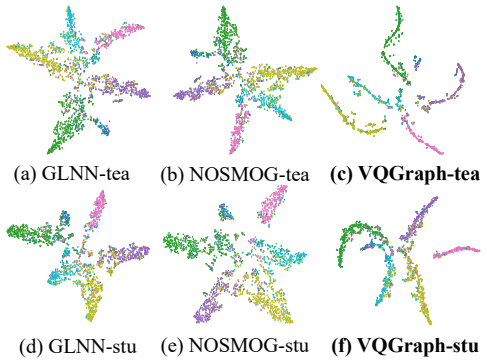

Figure 4: t-SNE visualization of learned node representations, colors denotes different classes.

unsuitable for real-world applications. This **makes VQGRAPH 105× faster than SAGE-L2 and 828× faster than SAGE-L3**. Although increasing the hidden size of NOSMOG slightly improves its performance, NOSMOGw2 (2-times wider than NOSMOG) and NOSMOGw4 still perform worse than VQGRAPH with more inference time, demonstrating the superior efficiency of our VQGRAPH.

Compactness of Learned Node Representation Space We use t-SNE (Van der Maaten & Hinton, 2008) to visualize the node representation spaces of both teacher GNN and distilled student MLP models with different methods, and put the results in Figure 4. Our VQGRAPH provides a better teacher GNN model than GLNN and NOSMOG, and the node representations of same classes have a more compact distribution. The representations extracted by our distilled MLP model also have a more compact distribution. We attribute these to our expressive code-based representation space, providing more structure-aware representations for classifying nodes. Besides, our new code-based distillation strategy can effectively deliver both graph structural information and categorial information from GNN to MLP, guaranteeing the compactness of MLP's representation space.

Consistency between Model Predictions and Global Graph Topology Here we corroborate the superiority of VQGRAPH over GNNs, MLPs, GLNN and NOSMOG in capturing global graph structural information, which is complementary to the above analysis on local structure awareness. We use the cut value to effectively evaluate the alignment between model predictions and graph topology as (Zhang et al., 2022b; Tian et al., 2023b) based on the approximation for the min-cut problem (Bianchi et al., 2019). The min-cut problem divides nodes $\mathcal{V}$ into K disjoint subsets by removing the minimum number of edges. Correspondingly, the min-cut problem can be expressed as: $\max \frac{1}{K}\sum_{k=1}^{K}(\boldsymbol{C}_k^T\boldsymbol{A}\boldsymbol{C}_k)/(\boldsymbol{C}_k^T\boldsymbol{D}\boldsymbol{C}_k)$, where $\boldsymbol{C}$ is the node class assignment, $\boldsymbol{A}$ is the adjacency matrix, and $\boldsymbol{D}$ is the degree matrix. Therefore, cut value is defined as follows: $\mathcal{CV} = tr(\hat{\boldsymbol{Y}}^T\boldsymbol{A}\hat{\boldsymbol{Y}})/tr(\hat{\boldsymbol{Y}}^T\boldsymbol{D}\hat{\boldsymbol{Y}})$, where $\hat{\boldsymbol{Y}}$ is the model prediction output, and the cut value $\mathcal{CV}$ indicates the consistency between the model predictions and the graph topology. We report the cut values for various models in the transductive setting in Tab. 3. The average $\mathcal{CV}$ achieved by VQGRAPH is **0.9493**, while SAGE, GLNN, and NOSMOG have average $\mathcal{CV}$ values of 0.9276, 0.8725, and 0.9348, respectively. We find VQGRAPH obtains the highest cut value, indicating the superior global structure-capturing ability over GNN and SOTA GNN-to-MLP distillation methods.

Table 3: The cut value. VQGRAPH predictions are more consistent with the graph topology than GNN, MLP, GLNN and the state-of-the-art method NOSMOG.

Datasets	SAGE	MLP	GLNN	NOSMOG	**VQGRAPH**
Citeseer	0.9535	0.8107	0.9447	0.9659	**0.9786**
Pubmed	0.9597	0.9062	0.9298	0.9641	**0.9883**
Cora	0.9385	0.7203	0.8908	0.9480	**0.9684**
A-computer	0.8951	0.6764	0.8579	0.9047	**0.9190**
A-photo	0.9014	0.7099	0.9063	0.9084	**0.9177**
Arxiv	0.9052	0.7252	0.8126	0.9066	**0.9162**
Products	0.9400	0.7518	0.7657	0.9456	**0.9571**
Average	0.9276	0.7572	0.8725	0.9348	**0.9493**

5.3 ABLATION STUDY

Influence of the Codebook Size We analyze the influence of the codebook size of our graph tokenizer. From Figure 5(i), we observe that changing codebook size can significantly influence the performance for our distilled MLP model. Too small a value can not have enough expressiveness

for preserving graph structures while too large a value will lead to code redundancy impairing the performance. Morever, VQGRAPH has different optimal codebook sizes for various datasets as in Figure 5(ii). Another interesting observation is the graph with more nodes or edges tends to require a larger codebook size to achieve optimal distillation results. In our VQGraph, the size of the codebook is mainly determined by the complexity of the graph data, considering both nodes and edges which produce different local substructures. Thus, our codebook size is still small compared to the exponential graph topological complexity, demonstrating the expressiveness of our codebook. Taking `Cora` as an example, our codebook size is 2048, but it contains 2485 nodes with an average degree about 4 which can theoretically result in $O(2485^4)$ possible 1-hop substructure patterns.

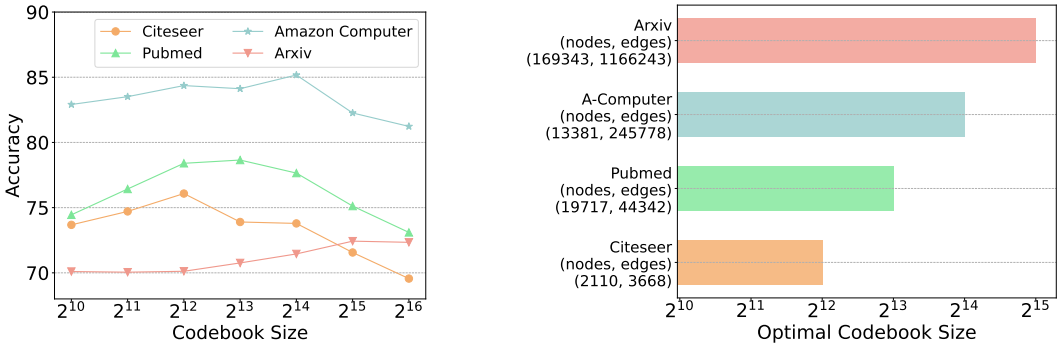

(i) Accuracy vs. Codebook Size. (ii) Optimal codebook size for various datasets.

Figure 5: Influence of the codebook size.

Contribution Analysis of VQGRAPH We design experiments to make statistical analysis on the contributions of our VQGRAPH. The results are presented in Tab. 4, and we observe that compared to traditional class-based distillation, both *Only-VQ* and VQGRAPH promote the average accuracy, suggesting that both graph tokenizer and soft code assignments have vital impacts on final performance. Moreover, comparing *AE+class-based* to *class-based*, we find adding structure awareness slightly improves GNN-to-MLP distillation. Our designed graph VQ-VAE efficiently improves the GNN-to-MLP distillation results more significantly than classic graph (Variational)AE, because we directly learn numerous structure-aware codes to enrich the expressiveness of node representations. Our *VQ+code-based* distillation (denoted as VQGRAPH) substantially improves node classification performance over *Only-VQ* across all datasets, demonstrating the superiority of our new structure-aware distillation targets over soft labels. Please refer to Appendix C for more ablation studies.

Table 4: *Class-based* denotes only using soft labels for distillation (e.g., GLNN), *AE+Class-based* denotes adding classic graph Auto-Encoder (Kipf & Welling, 2016) for structure awareness. *Only-VQ* denotes using VQ for training teacher but using soft labels for distillation. $\Delta_{\text{Only-VQ}}$, Δ_{VQGRAPH} represents the differences between Only-VQ, VQGRAPH and *Class-based*.

Datasets	GNN	Class-based	AE+Class-based	**Only-VQ (ours)**	**VQGRAPH (ours)**	$\Delta_{\text{Only-VQ}}$	Δ_{VQGRAPH}
`Citeseer`	70.49 ± 1.53	71.22 ± 1.54	71.65 ± 0.69	$\mathbf{74.96 \pm 1.50}$	$\mathbf{76.08 \pm 0.55}$	$\uparrow 5.25\%$	$\uparrow 6.82\%$
`Pubmed`	75.56 ± 2.06	75.59 ± 2.46	76.56 ± 1.23	$\mathbf{77.86 \pm 2.46}$	$\mathbf{78.40 \pm 1.71}$	$\uparrow 3.00\%$	$\uparrow 3.71\%$
`Cora`	80.64 ± 1.57	80.26 ± 1.66	81.11 ± 1.01	$\mathbf{82.48 \pm 0.46}$	$\mathbf{83.93 \pm 0.87}$	$\uparrow 2.77\%$	$\uparrow 4.57\%$
`A-computer`	82.82 ± 1.37	82.71 ± 1.18	83.01 ± 1.18	$\mathbf{84.06 \pm 1.18}$	$\mathbf{85.17 \pm 1.29}$	$\uparrow 1.63\%$	$\uparrow 2.97\%$
`A-photo`	90.85 ± 0.87	91.95 ± 1.04	92.06 ± 0.69	$\mathbf{93.86 \pm 1.04}$	$\mathbf{94.21 \pm 0.45}$	$\uparrow 2.08\%$	$\uparrow 2.45\%$
`Arxiv`	70.73 ± 0.35	63.75 ± 0.48	70.10 ± 1.02	$\mathbf{70.75 \pm 0.48}$	$\mathbf{72.43 \pm 0.20}$	$\uparrow 10.98\%$	$\uparrow 13.61\%$
`Products`	77.17 ± 0.32	67.71 ± 0.31	77.65 ± 0.98	$\mathbf{78.71 \pm 0.31}$	$\mathbf{79.17 \pm 0.21}$	$\uparrow 16.25\%$	$\uparrow 16.93\%$

6 CONCLUSION

In this paper, we improve the expressiveness of existing graph representation space by directly labeling nodes' diverse local structures with a codebook, and utilizing the codebook for facilitating structure-aware GNN-to-MLP distillation. Extensive experiments on seven datasets demonstrate that our VQGRAPH can significantly improve GNNs by **3.90%**, MLPs by **28.05%**, and the state-of-the-art GNN-to-MLP distillation method by **1.39%** on average accuracy, while maintaining a fast inference speed of **828×** compared to GNNs. Furthermore, we present additional visualization and statistical analyses as well as ablation studies to demonstrate the superiority of the proposed model.

ACKNOWLEDGEMENT

This work was supported by the National Natural Science Foundation of China (No.61832001 and U22B2037).

REFERENCES

Sami Abu-El-Haija, Bryan Perozzi, Amol Kapoor, Nazanin Alipourfard, Kristina Lerman, Hrayr Harutyunyan, Greg Ver Steeg, and Aram Galstyan. Mixhop: Higher-order graph convolutional architectures via sparsified neighborhood mixing. In *international conference on machine learning*, pp. 21–29. PMLR, 2019.

Yoshua Bengio, Nicholas Léonard, and Aaron Courville. Estimating or propagating gradients through stochastic neurons for conditional computation. *arXiv preprint arXiv:1308.3432*, 2013.

Filippo Maria Bianchi, Daniele Grattarola, and Cesare Alippi. Mincut pooling in graph neural networks. 2019.

Aleksandar Bojchevski, Johannes Gasteiger, Bryan Perozzi, Amol Kapoor, Martin Blais, Benedek Rózemberczki, Michal Lukasik, and Stephan Günnemann. Scaling graph neural networks with approximate pagerank. In *Proceedings of the 26th ACM SIGKDD International Conference on Knowledge Discovery & Data Mining*, pp. 2464–2473, 2020.

H Bunke and G Allermann. Inexact graph matching for structural pattern recognition. *Pattern Recognition Letters*, 1(4):245–253, 1983. ISSN 0167-8655. doi: https://doi.org/10.1016/0167-8655(83)90033-8. URL https://www.sciencedirect.com/science/article/pii/0167865583900338.

Jianfei Chen, Jun Zhu, and Le Song. Stochastic training of graph convolutional networks with variance reduction. In *International Conference on Machine Learning*, pp. 942–950. PMLR, 2018a.

Jie Chen, Tengfei Ma, and Cao Xiao. Fastgcn: Fast learning with graph convolutional networks via importance sampling. In *International Conference on Learning Representations*, 2018b.

Jie Chen, Tengfei Ma, and Cao Xiao. FastGCN: Fast learning with graph convolutional networks via importance sampling. In *International Conference on Learning Representations*, 2018c.

Ming Chen, Zhewei Wei, Bolin Ding, Yaliang Li, Ye Yuan, Xiaoyong Du, and Ji-Rong Wen. Scalable graph neural networks via bidirectional propagation. *Advances in neural information processing systems*, 33:14556–14566, 2020a.

Ming Chen, Zhewei Wei, Zengfeng Huang, Bolin Ding, and Yaliang Li. Simple and deep graph convolutional networks. In *ICML*, 2020b.

Ming Chen, Zhewei Wei, Zengfeng Huang, Bolin Ding, and Yaliang Li. Simple and deep graph convolutional networks, 2020c.

Yu-Hsin Chen, Joel Emer, and Vivienne Sze. Eyeriss: A spatial architecture for energy-efficient dataflow for convolutional neural networks. In *2016 ACM/IEEE 43rd Annual International Symposium on Computer Architecture (ISCA)*, pp. 367–379, 2016. doi: 10.1109/ISCA.2016.40.

Wei-Lin Chiang, Xuanqing Liu, Si Si, Yang Li, Samy Bengio, and Cho-Jui Hsieh. Cluster-gcn: An efficient algorithm for training deep and large graph convolutional networks. In *Proceedings of the 25th ACM SIGKDD international conference on knowledge discovery & data mining*, pp. 257–266, 2019.

Eli Chien, Wei-Cheng Chang, Cho-Jui Hsieh, Hsiang-Fu Yu, Jiong Zhang, Olgica Milenkovic, and Inderjit S Dhillon. Node feature extraction by self-supervised multi-scale neighborhood prediction. In *International Conference on Learning Representations*, 2022.

Xiang Deng and Zhongfei Zhang. Graph-free knowledge distillation for graph neural networks, 2021.

Yingtong Dou, Zhiwei Liu, Li Sun, Yutong Deng, Hao Peng, and Philip S Yu. Enhancing graph neural network-based fraud detectors against camouflaged fraudsters. In *Proceedings of the 29th ACM International Conference on Information & Knowledge Management*, pp. 315–324, 2020.

Wenqi Fan, Yao Ma, Qing Li, Yuan He, Eric Zhao, Jiliang Tang, and Dawei Yin. Graph neural networks for social recommendation. In *The world wide web conference*, pp. 417–426, 2019.

Matthias Fey, Jan E Lenssen, Frank Weichert, and Jure Leskovec. Gnnautoscale: Scalable and expressive graph neural networks via historical embeddings. In *International Conference on Machine Learning*, pp. 3294–3304. PMLR, 2021.

Xinbo Gao, Bing Xiao, Dacheng Tao, and Xuelong Li. A survey of graph edit distance. *Pattern Anal. Appl.*, 13:113–129, 02 2010. doi: 10.1007/s10044-008-0141-y.

Jianping Gou, Baosheng Yu, Stephen J Maybank, and Dacheng Tao. Knowledge distillation: A survey. *International Journal of Computer Vision*, 2021.

Qingyu Guo, Fuzhen Zhuang, Chuan Qin, Hengshu Zhu, Xing Xie, Hui Xiong, and Qing He. A survey on knowledge graph-based recommender systems. *IEEE Transactions on Knowledge and Data Engineering*, 34(8):3549–3568, 2020.

Suyog Gupta, Ankur Agrawal, Kailash Gopalakrishnan, and Pritish Narayanan. Deep learning with limited numerical precision. In Francis Bach and David Blei (eds.), *Proceedings of the 32nd International Conference on Machine Learning*, volume 37 of *Proceedings of Machine Learning Research*, pp. 1737–1746, Lille, France, 07–09 Jul 2015. PMLR.

William L. Hamilton, Rex Ying, and Jure Leskovec. Inductive representation learning on large graphs. In *NeurIPS*, 2017.

Song Han, Jeff Pool, John Tran, and William J. Dally. Learning both weights and connections for efficient neural networks. In *Proceedings of the 28th International Conference on Neural Information Processing Systems - Volume 1*, NIPS'15, pp. 1135–1143, Cambridge, MA, USA, 2015. MIT Press.

Xiangnan He, Kuan Deng, Xiang Wang, Yan Li, Yongdong Zhang, and Meng Wang. Lightgcn: Simplifying and powering graph convolution network for recommendation. In *Proceedings of the 43rd International ACM SIGIR conference on research and development in Information Retrieval*, pp. 639–648, 2020.

Geoffrey Hinton, Oriol Vinyals, Jeff Dean, et al. Distilling the knowledge in a neural network. *arXiv preprint arXiv:1503.02531*, 2015.

Weihua Hu, Matthias Fey, Marinka Zitnik, Yuxiao Dong, Hongyu Ren, Bowen Liu, Michele Catasta, and Jure Leskovec. Open graph benchmark: Datasets for machine learning on graphs. *Advances in neural information processing systems*, 33:22118–22133, 2020a.

Weihua Hu, Matthias Fey, Marinka Zitnik, Yuxiao Dong, Hongyu Ren, Bowen Liu, Michele Catasta, and Jure Leskovec. Open graph benchmark: Datasets for machine learning on graphs. *CoRR*, abs/2005.00687, 2020b.

Yang Hu, Haoxuan You, Zhecan Wang, Zhicheng Wang, Erjin Zhou, and Yue Gao. Graph-mlp: node classification without message passing in graph. *arXiv preprint arXiv:2106.04051*, 2021.

Qian Huang, Horace He, Abhay Singh, Ser-Nam Lim, and Austin Benson. Combining label propagation and simple models out-performs graph neural networks. In *International Conference on Learning Representations*, 2021.

Wenbing Huang, Tong Zhang, Yu Rong, and Junzhou Huang. Adaptive sampling towards fast graph representation learning. *Advances in neural information processing systems*, 31, 2018.

Zhihao Jia, Sina Lin, Rex Ying, Jiaxuan You, Jure Leskovec, and Alex Aiken. Redundancy-free computation for graph neural networks. In *Proceedings of the 26th ACM SIGKDD International Conference on Knowledge Discovery & Data Mining*, pp. 997–1005, 2020.

Patrick Judd, Jorge Albericio, Tayler Hetherington, Tor M. Aamodt, Natalie Enright Jerger, and Andreas Moshovos. Proteus: Exploiting numerical precision variability in deep neural networks. In *Proceedings of the 2016 International Conference on Supercomputing*, pp. 23, 2016.

Thomas N Kipf and Max Welling. Variational graph auto-encoders. *arXiv preprint arXiv:1611.07308*, 2016.

Thomas N. Kipf and Max Welling. Semi-supervised classification with graph convolutional networks. In *ICLR*, 2017.

Johannes Klicpera, Aleksandar Bojchevski, and Stephan Günnemann. Predict then propagate: Graph neural networks meet personalized pagerank. In *ICLR*, 2019.

Yonghyeon Lee, Hyeokjun Kwon, and Frank Park. Neighborhood reconstructing autoencoders. *Advances in Neural Information Processing Systems*, 34:536–546, 2021.

Guohao Li, Matthias Muller, Ali Thabet, and Bernard Ghanem. Deepgcns: Can gcns go as deep as cnns? In *ICCV*, 2019.

Pan Li, Yanbang Wang, Hongwei Wang, and Jure Leskovec. Distance encoding: Design provably more powerful neural networks for graph representation learning. In *NeurIPS*, 2020a.

Xiangsheng Li, Maarten de Rijke, Yiqun Liu, Jiaxin Mao, Weizhi Ma, Min Zhang, and Shaoping Ma. Learning better representations for neural information retrieval with graph information. In *Proceedings of the 29th ACM International Conference on Information & Knowledge Management*, pp. 795–804, 2020b.

Yang Liu, Xiang Ao, Zidi Qin, Jianfeng Chi, Jinghua Feng, Hao Yang, and Qing He. Pick and choose: a gnn-based imbalanced learning approach for fraud detection. In *Proceedings of the Web Conference 2021*, pp. 3168–3177, 2021.

Sitao Luan, Chenqing Hua, Qincheng Lu, Jiaqi Zhu, Mingde Zhao, Shuyuan Zhang, Xiao-Wen Chang, and Doina Precup. Revisiting heterophily for graph neural networks, 2022.

Kelong Mao, Xi Xiao, Jieming Zhu, Biao Lu, Ruiming Tang, and Xiuqiang He. Item tagging for information retrieval: a tripartite graph neural network based approach. In *Proceedings of the 43rd International ACM SIGIR Conference on Research and Development in Information Retrieval*, pp. 2327–2336, 2020.

Christopher Morris, Martin Ritzert, Matthias Fey, William L Hamilton, Jan Eric Lenssen, Gaurav Rattan, and Martin Grohe. Weisfeiler and leman go neural: Higher-order graph neural networks. In *AAAI*, 2019.

Galileo Namata, Ben London, Lise Getoor, Bert Huang, and U Edu. Query-driven active surveying for collective classification. In *10th international workshop on mining and learning with graphs*, volume 8, pp. 1, 2012.

Joonhyung Park, Jaeyun Song, and Eunho Yang. Graphens: Neighbor-aware ego network synthesis for class-imbalanced node classification. In *International Conference on Learning Representations*, 2021.

Hongbin Pei, Bingzhe Wei, Kevin Chen-Chuan Chang, Yu Lei, and Bo Yang. Geom-gcn: Geometric graph convolutional networks. *CoRR*, abs/2002.05287, 2020a.

Hongbin Pei, Bingzhe Wei, Kevin Chen-Chuan Chang, Yu Lei, and Bo Yang. Geom-gcn: Geometric graph convolutional networks. In *International Conference on Learning Representations*, 2020b.

Bryan Perozzi, Rami Al-Rfou, and Steven Skiena. Deepwalk: Online learning of social representations. In *KDD*, 2014.

Alberto Sanfeliu and King-Sun Fu. A distance measure between attributed relational graphs for pattern recognition. *IEEE Transactions on Systems, Man, and Cybernetics*, SMC-13(3):353–362, 1983. doi: 10.1109/TSMC.1983.6313167.

Prithviraj Sen, Galileo Namata, Mustafa Bilgic, Lise Getoor, Brian Galligher, and Tina Eliassi-Rad. Collective classification in network data. *AI magazine*, 29(3):93–93, 2008.

Rico Sennrich, Barry Haddow, and Alexandra Birch. Neural machine translation of rare words with subword units. In *Proceedings of the 54th Annual Meeting of the Association for Computational Linguistics (Volume 1: Long Papers)*, pp. 1715–1725, 2016.

Oleksandr Shchur, Maximilian Mumme, Aleksandar Bojchevski, and Stephan Günnemann. Pitfalls of graph neural network evaluation. *arXiv preprint arXiv:1811.05868*, 2018.

Zhihao Shi, Xize Liang, and Jie Wang. Lmc: Fast training of gnns via subgraph sampling with provable convergence. In *The Eleventh International Conference on Learning Representations*, 2023.

Mingyue Tang, Pan Li, and Carl Yang. Graph auto-encoder via neighborhood wasserstein reconstruction. In *International Conference on Learning Representations*, 2022.

Yijun Tian, Shichao Pei, Xiangliang Zhang, Chuxu Zhang, and Nitesh V Chawla. Knowledge distillation on graphs: A survey. *arXiv preprint arXiv:2302.00219*, 2023a.

Yijun Tian, Chuxu Zhang, Zhichun Guo, Xiangliang Zhang, and Nitesh Chawla. Learning mlps on graphs: A unified view of effectiveness, robustness, and efficiency. In *The Eleventh International Conference on Learning Representations*, 2023b.

Aaron Van Den Oord, Oriol Vinyals, et al. Neural discrete representation learning. *Advances in neural information processing systems*, 30, 2017.

Laurens Van der Maaten and Geoffrey Hinton. Visualizing data using t-sne. *Journal of machine learning research*, 9(11), 2008.

Petar Veličković, Guillem Cucurull, Arantxa Casanova, Adriana Romero, Pietro Liò, and Yoshua Bengio. Graph attention networks. In *ICLR*, 2018.

Shiwen Wu, Fei Sun, Wentao Zhang, Xu Xie, and Bin Cui. Graph neural networks in recommender systems: a survey. *ACM Computing Surveys*, 55(5):1–37, 2022.

Yonghui Wu, Mike Schuster, Zhifeng Chen, Quoc V Le, Mohammad Norouzi, Wolfgang Macherey, Maxim Krikun, Yuan Cao, Qin Gao, Klaus Macherey, et al. Google's neural machine translation system: Bridging the gap between human and machine translation. *arXiv preprint arXiv:1609.08144*, 2016.

Zonghan Wu, Shirui Pan, Fengwen Chen, Guodong Long, Chengqi Zhang, and S Yu Philip. A comprehensive survey on graph neural networks. *IEEE transactions on neural networks and learning systems*, 2020.

Keyulu Xu, Weihua Hu, Jure Leskovec, and Stefanie Jegelka. How powerful are graph neural networks? In *ICLR*, 2019.

Yishi Xu, Yingxue Zhang, Wei Guo, Huifeng Guo, Ruiming Tang, and Mark Coates. Graphsail: Graph structure aware incremental learning for recommender systems. In *Proceedings of the 29th ACM International Conference on Information; Knowledge Management*, CIKM '20, pp. 2861–2868, New York, NY, USA, 2020. Association for Computing Machinery. ISBN 9781450368599. doi: 10.1145/3340531.3412754.

Bencheng Yan, Chaokun Wang, Gaoyang Guo, and Yunkai Lou. Tinygnn: Learning efficient graph neural networks. In *Proceedings of the 26th ACM SIGKDD International Conference on Knowledge Discovery & Data Mining (KDD)*, pp. 1848–1856, 2020.

Cheng Yang, Jiawei Liu, and Chuan Shi. Extract the knowledge of graph neural networks and go beyond it: An effective knowledge distillation framework. In *WWW*, 2021a.

Cheng Yang, Jiawei Liu, and Chuan Shi. Extract the knowledge of graph neural networks and go beyond it: An effective knowledge distillation framework, 2021b.

Ling Yang and Shenda Hong. Omni-granular ego-semantic propagation for self-supervised graph representation learning. In *International Conference on Machine Learning*, pp. 25022–25037. PMLR, 2022.

Yiding Yang, Jiayan Qiu, Mingli Song, Dacheng Tao, and Xinchao Wang. Distilling knowledge from graph convolutional networks, 2021c.

Rex Ying, Ruining He, Kaifeng Chen, Pong Eksombatchai, William L Hamilton, and Jure Leskovec. Graph convolutional neural networks for web-scale recommender systems. In *Proceedings of the 24th ACM SIGKDD international conference on knowledge discovery & data mining*, pp. 974–983, 2018.

Li Yuan, Francis EH Tay, Guilin Li, Tao Wang, and Jiashi Feng. Revisiting knowledge distillation via label smoothing regularization. In *Proceedings of the IEEE/CVF Conference on Computer Vision and Pattern Recognition*, pp. 3903–3911, 2020.

Hanqing Zeng, Hongkuan Zhou, Ajitesh Srivastava, Rajgopal Kannan, and Viktor Prasanna. Graph-saint: Graph sampling based inductive learning method, 2020.

Chunhui Zhang, Chao Huang, Yijun Tian, Qianlong Wen, Zhongyu Ouyang, Youhuan Li, Yanfang Ye, and Chuxu Zhang. Diving into unified data-model sparsity for class-imbalanced graph representation learning. In *GLFrontiers*, 2022a.

Dalong Zhang, Xin Huang, Ziqi Liu, Zhiyang Hu, Xianzheng Song, Zhibang Ge, Zhiqiang Zhang, Lin Wang, Jun Zhou, Yang Shuang, et al. Agl: A scalable system for industrial-purpose graph machine learning. *arXiv preprint arXiv:2003.02454*, 2020.

Shichang Zhang, Yozen Liu, Yizhou Sun, and Neil Shah. Graph-less neural networks: Teaching old mlps new tricks via distillation. In *ICLR*, 2022b.

Lingxiao Zhao, Wei Jin, Leman Akoglu, and Neil Shah. From stars to subgraphs: Uplifting any gnn with local structure awareness. In *International Conference on Learning Representations*, 2022.

Yiren Zhao, Duo Wang, Daniel Bates, Robert Mullins, Mateja Jamnik, and Pietro Lio. Learned low precision graph neural networks, 2020.

Wenqing Zheng, Edward W Huang, Nikhil Rao, Sumeet Katariya, Zhangyang Wang, and Karthik Subbian. Cold brew: Distilling graph node representations with incomplete or missing neighborhoods. In *ICLR*, 2022.

Helong Zhou and Liangchen Song. Rethinking soft labels for knowledge distillation: A bias–variance tradeoff perspective. In *Proceedings of International Conference on Learning Representations (ICLR)*, 2021.

Hongkuan Zhou, Ajitesh Srivastava, Hanqing Zeng, Rajgopal Kannan, and Viktor K. Prasanna. Accelerating large scale real-time GNN inference using channel pruning. *CoRR*, abs/2105.04528, 2021.

Jie Zhou, Ganqu Cui, Shengding Hu, Zhengyan Zhang, Cheng Yang, Zhiyuan Liu, Lifeng Wang, Changcheng Li, and Maosong Sun. Graph neural networks: A review of methods and applications. *AI Open*, 2020.

Jiong Zhu, Yujun Yan, Lingxiao Zhao, Mark Heimann, Leman Akoglu, and Danai Koutra. Beyond homophily in graph neural networks: Current limitations and effective designs, 2020.

Qi Zhu, Carl Yang, Yidan Xu, Haonan Wang, Chao Zhang, and Jiawei Han. Transfer learning of graph neural networks with ego-graph information maximization. *Advances in Neural Information Processing Systems*, 34:1766–1779, 2021.

Xiaojin Zhu and Zoubin Ghahramanih. Learning from labeled and unlabeled data with label propagation. 2002.

Difan Zou, Ziniu Hu, Yewen Wang, Song Jiang, Yizhou Sun, and Quanquan Gu. Layer-dependent importance sampling for training deep and large graph convolutional networks. *arXiv preprint arXiv:1911.07323*, 2019.

A More Analysis and Results

A.1 Connection between Local Graph Structure and Learned Codebook

To better illustrate the connection between local graph structure and the codebook learned by our graph VQ-VAE, we conduct node-centered subgraph retrieval in the learned MLP representation spaces of NOSMOG and our VQGraph. Specifically, we extract the representation with distilled MLP model for a query node in `Citeseer`. We demonstrate 4 subgraphs centered at the nodes that are most similar to the query node representation with the cosine similarities in the whole graph in Figure 6. As can be observed, the identical token IDs yield similar substructures, indicating the representation similarities of VQGraph are approximately aligned with the local subgraph similarities, which is denoted as graph edit distance (GED) Sanfeliu & Fu (1983); Bunke & Allermann (1983); Gao et al. (2010) and is one of the most popular graph matching methods. In contrast, the representations extracted from NOSMOG fail to sufficiently model and reflect the structural similarities between subgraphs. Hence, VQGraph is necessary and effective for addressing structure-complex graph tasks. Moreover, we observe that VQGraph can be aware of the minor neighborhood structural difference despite the nodes with the same class, demonstrating the more fine-grained expressiveness of our token-based distillation, which further helps with more accurate classification.

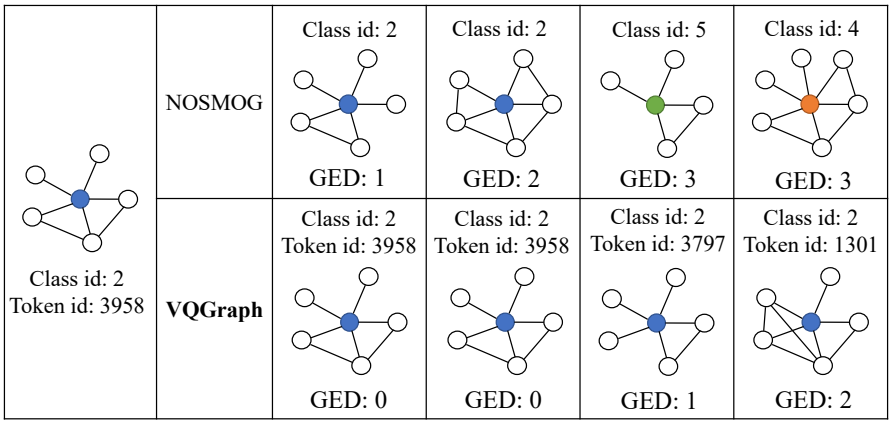

Figure 6: The query node and 4 closest nodes in distilled MLP representation space with corresponding subgraphs.

A.2 VQGraph for Heterophilic Graphs

In addition to homophilic graphs, we extend our proposed method to heterophilic graphs for further evaluation. We consider 2 heterophilic datasets, `Texas` and `Cornell`, realsed by Pei et al. (2020a). `Texas` and `Cornell` are web page datasets collected from computer science departments of various universities. In these datasets, nodes are web pages and edges represent hyperlinks between them. Bag-of-words representations are taken as nodes' feature vectors. The task is to classify the web pages into five categories including student, project, course, staff and faculty. Basic statistics of the datasets are shown in Tab. 5. The Edge Hom. (Zhu et al. (2020)) is defined as the fraction of edges that connect nodes with the same label.

Table 5: Heterophilic Dataset Statistics.

Dataset	# Nodes	# Edges	# Features	# Classes	# Edge Hom.
`Texas`	183	295	1,703	5	0.11
`Cornell`	183	280	1,703	5	0.30

We incorporate our structure-aware code embeddings with two state-of-the-art GNN models known for their efficacy on heterophilic graphs, namely ACMGCN (Luan et al. (2022)) and GCNII (Chen

et al. (2020c)), along with MLP. We compare with these baselines in Tab. 6. The results of these experiments demonstrate that our graph VQ-VAE can generalize to different heterophilic GNN/MLP architectures and consistently improve their performances.

Table 6: Results on Heterophilic Graphs.

	Texas	**Cornell**
ACMGCN	86.49	84.05
ACMGCN with our Graph VQ-VAE	**87.03**	**84.59**
MLP	75.68	76.38
MLP with our Graph VQ-VAE	**77.93**	**78.29**
GCNII	76.73	76.49
GCNII with our Graph VQ-VAE	**79.04**	**78.29**

A.3 Analysis on Codebook Entries

In the training stage, we tokenize each node with different neighborhood structures as discrete codes using Graph VQ-VAE. Now we take a closer look at codebook entries for different classes on Pubmed for in-depth analysis (Tabs. 7 and 8). There is little difference in the number of codes with each class and there is a uniform distribution of the nodes for each class, demonstrating the learning capacity of our model. Meanwhile, the results demonstrate that there is a small code overlap among different classes, which indicates the code distributions learned for different classes are mutually independent. This finding validates that our graph VQ-VAE enables distinct separation of the nodes with different class labels in the representation space, facilitating a better knowledge transfer in GNN-to-MLP distillation.

Table 7: Codebook Entries for Each Class in `Pubmed`.

	Class 1	Class 2	Class 3
Code Entries	2,560	2,623	2,591

Table 8: The Overlapping Codes (%) for Each Paired Classes of `Pubmed`.

	Class 1	Class 2	Class 3
Class 1	*	0.9%	0.8%
Class 2		*	0.6%
Class 3			*

B Experiment Details

B.1 Datasets

The statistics of the seven public benchmark datasets used in our experiments are shown in Tab. 9. For all datasets, we follow the setting in the original paper to split the data. Specifically, for the five small datasets (i.e., Cora, Citeseer, Pubmed, A-computer, and A-photo), we use the splitting strategy in the CPF paper (Yang et al., 2021b), where each random seed corresponding to a different split. For the two OGB large datasets (i.e., Arxiv and Products), we follow the official splits in Hu et al. (2020a) based on time and popularity, respectively. We introduce each dataset as follows:

- `Citeseer` (Sen et al., 2008) is a benchmark citation dataset consisting of scientific publications, with the configuration similar to the Cora dataset. The dictionary contains 3,703 unique words. Citeseer dataset has the largest number of features among all datasets used in this paper.

- `Pubmed` (Namata et al., 2012) is a citation benchmark consisting of diabetes-related articles from the PubMed database. The node features are TF/IDF-weighted word frequency, and the label indicates the type of diabetes covered in this article.
- `Cora` (Sen et al., 2008) is a benchmark citation dataset composed of scientific publications. Each node in the graph represents a publication whose feature vector is a sparse bag-of-words with 0/1-values indicating the absence/presence of the corresponding word from the word dictionary. Edges represent citations between papers, and labels indicate the research field of each paper.
- `A-computer` and `A-photo` (Shchur et al., 2018) are two benchmark datasets that are extracted from Amazon co-purchase graph. Nodes represent products, edges indicate whether two products are frequently purchased together, features represent product reviews encoded by bag-of-words, and labels are predefined product categories.
- `Arxiv` (Hu et al., 2020a) is a benchmark citation dataset composed of Computer Science arXiv papers. Each node is an arXiv paper and each edge indicates that one paper cites another one. The node features are average word embeddings of the title and abstract.
- `Products` (Hu et al., 2020a) is a benchmark Amazon product co-purchasing network dataset. Nodes represent products sold on Amazon, and edges between two products indicate that the products are purchased together. The node features are bag-of-words features from the product descriptions.

Table 9: Dataset Statistics.

Dataset	# Nodes	# Edges	# Features	# Classes
`Citeseer`	2,110	3,668	3,703	6
`Pubmed`	19,717	44,324	500	3
`Cora`	2,485	5,069	1,433	7
`A-computer`	13,381	245,778	767	10
`A-photo`	7,487	119,043	745	8
`Arxiv`	169,343	1,166,243	128	40
`Products`	2,449,029	61,859,140	100	47

B.2 Model Hyperparameters and Implementation Details

The code and trained models are provided in the supplementary material.

Production Scenario Regarding to the production scenario, we recognize that real-world deployment of models necessitates the ability to generate predictions for new data points as well as reliably maintain performance on existing ones. Therefore, we apply our method in a realistic production setting to better understand the effectiveness of GNN-to-MLP models, encompassing both transductive and inductive predictions. In a real-life production environment, it is common for a model to be retrained periodically. The holdout nodes in the inductive set represent new nodes that have entered the graph between two training periods. To mitigate potential randomness and to evaluate generalizability more effectively, we employ a test dataset V_{ind}^{U}, which contains 20% of the test data, and another dataset V_{obs}^{U}, containing the remaining 80% of the test data. This setup allows us to evaluate the model's performance on both observed unlabeled nodes (transductive prediction) and newly introduced nodes (inductive prediction), reflecting real-world inference scenarios. We further provide three sets of results: "tran" refers to results on V_{obs}^{U}, "ind" refers to V_{ind}^{U}, and "prod" refers to an interpolated value between tran and ind, according to the split rate, indicating the performance in real production settings.

Graph Tokenizer Pre-Training We first train our graph tokenizer which contains a teacher GNN model and a learnable codebook, then use both the GNN and the codebook to conduct GNN-to-MLP distillation. The hyperparameters of GNN models on each dataset are taken from the best hyperparameters provided by the CPF paper (Yang et al., 2021b) (Tab. 10) and the OGB official examples (Hu et al., 2020a) (Tab. 11). We provide the hyperparameters of our codebooks for different datasets

in Tab. 12. Kindly note that the VQ procedure is inserted between the encoder and the classifier of the GNN model, and the dimensions of code embedding and GNN feature are same for convenient assignment. And the code embeddings are initialized with uniform distribution. During the training of our graph tokenizer, VQGRAPH additionally includes two separate linear decoder layers to decode node attributes and graph topology, respectively, based on assigned code embeddings.

Code-Based GNN-to-MLP Distillation We freeze the parameters of both the pre-trained teacher GNN model and the learned codebook embeddings for our code-based GNN-to-MLP distillation. For the student MLP in VQGRAPH, unless otherwise specified with -wi or -Li, we set the number of layers and the hidden dimension of each layer to be the same as the teacher GNN, so their total number of parameters stays the same as the teacher GNN (in Tab. 12). In distillation, the teacher GNN not only delivers the soft labels with respect to node classification to the MLP, but also produces its corresponding soft code assignment for the MLP. Kindly recall that we use codebook embeddings to compute code assignments for the MLP only in training process, and we remove this assigning procedure for deploying the distilled MLP in testing process, which does not increase inference time. In practice, categorial and structural information might be of different importance to the distillation in various graph datasets. We correspondingly modify their loss weights for better performance.

Table 10: Hyperparameters for GNNs on five datasets from the CPF paper.

	SAGE	GCN	GAT	APPNP
# layers	2	2	2	2
hidden dim	128	64	64	64
learning rate	0.01	0.01	0.01	0.01
weight decay	0.0005	0.001	0.01	0.01
dropout	0	0.8	0.6	0.5
fan out	5,5	-	-	-
attention heads	-	-	8	-
power iterations	-	-	-	10

Table 11: Hyperparameters for GraphSAGE on OGB datasets.

Dataset	Arxiv	Products
# layers	3	3
hidden dim	256	256
learning rate	0.01	0.003
weight decay	0	0
dropout	0.2	0.5
normalization	batch	batch
fan out	[5, 10, 15]	[5, 10, 15]

Table 12: Hyperparameters of VQGRAPH.

	Citeseer	Pubmed	Cora	A-computer	A-photo	Arxiv	Products
tokenizer attribute decoder layers	1	1	1	1	1	1	1
tokenizer topology decoder layers	1	1	1	1	1	1	1
codebook size	4096	8192	2048	16384	8192	32768	32,768
τ in $\mathcal{L}_{code_distill}$	4	4	4	4	4	4	4
MLP layers	2	2	2	2	2	3	3
hidden dim	128	128	128	128	128	256	256
learning rate	0.01	0.01	0.005	0.003	0.001	0.01	0.003
weight decay	0.005	0.001	0.001	0.005	0.001	0	0
dropout	0.6	0.1	0.4	0.1	0.1	0.2	0.5
α for $\mathcal{L}_{class_distill}$	1	1	1	1	1	1	1
β for $\mathcal{L}_{code_distill}$	1e-8	1e-8	1e-8	1e-8	1e-8	1e-8	1e-8

C More Ablation Studies

C.1 VQGraph with Different Relation Modules in Equation (4)

In Sec. 4.2, we compute 1-*vs*-M token-wise relations in Equation (4) using L_2 distance as the relation module COMP$(\cdot,\cdot)$. Other relation modules can also be applied, and we thus conduct experiments based on cosine similarity with the results depicted in Tab. 13. Experiments across different datasets illustrate that VQGraph with different relation modules can consistently improve the code distillation performance of VQGraph. The influence of relation module on VQGraph's overall performance is very minimal, with L_2 distance exhibiting a slight advantage of approximately 0.2% on average accuracy.

Table 13: VQGraph with diffrent relation modules.

Datasets	GNN	w/ Cosine Similarity	**w/ L_2 distance**	Δ
`Citeseer`	70.49 ± 1.53	75.80 ± 0.66	$\mathbf{76.08 \pm 0.55}$	$\uparrow 0.12\%$
`Pubmed`	75.56 ± 2.06	78.12 ± 1.23	$\mathbf{78.40 \pm 1.71}$	$\uparrow 0.23\%$
`Cora`	80.64 ± 1.57	83.61 ± 0.70	$\mathbf{83.93 \pm 0.87}$	$\uparrow 0.20\%$
`A-computer`	82.82 ± 1.37	84.96 ± 1.06	$\mathbf{85.17 \pm 1.29}$	$\uparrow 0.20\%$
`A-photo`	90.85 ± 0.87	94.05 ± 0.29	$\mathbf{94.21 \pm 0.45}$	$\uparrow 0.18\%$
`Arxiv`	70.73 ± 0.35	71.96 ± 0.18	$\mathbf{72.43 \pm 0.20}$	$\uparrow 0.16\%$
`Products`	77.17 ± 0.32	79.01 ± 0.34	$\mathbf{79.17 \pm 0.21}$	$\uparrow 0.18\%$

C.2 VQGraph with Different Teacher GNNs

In VQGraph, we utilize GraphSAGE with GCN aggregation to represent our teacher GNN. However, given that different GNN architectures may exhibit varying performance across datasets, we seek to investigate whether VQGraph can perform well when trained with other GNN architectures. As displayed in Figure 7, we present the average performance of VQGraph when distilled from different teacher GNNs, including GCN, GAT, and APPNP, across five benchmark datasets. Our results demonstrate that all four teacher models achieved comparable performance, but VQGraph consistently outperforms teacher GNNs and other GNN-to-MLP distillation methods, indicating the superior effectiveness and generalization ability of our VQGraph.

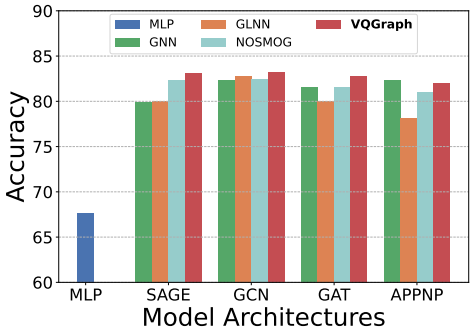

Figure 7: Accuracy vs. Teacher GNN Model Architectures.

C.3 Robustness Evaluation with Noisy Features

We evaluate the robustness of VQGraph with regards to different noise levels across different datasets and compute average accuracy. Specifically, we follow Tian et al. (2023b) to initialize the node features and introduce different levels of Gaussian noises to the node features by modifying $\boldsymbol{X}$ with $\tilde{\boldsymbol{X}} = (1-\alpha)\cdot\boldsymbol{X}+\alpha\cdot n$, where n denotes an independent Gaussian noise and $\alpha \in [0,1]$ controls the noise level. Our results, as illustrated in Figure 8, reveal that VQGraph achieves comparable or improved performance compared to GNNs and previous SOTA NOSMOG across different levels

of noise, demonstrating its superior noise-robustness and efficacy, especially when GNNs leverage local structure information of subgraphs to mitigate noise impact. Conversely, GLNN and MLP exhibit rapid performance deterioration as α increases. In the extreme case where α equals 1, and the input features are entirely perturbed, resulting in $\tilde{\boldsymbol{X}}$ and $\boldsymbol{X}$ being independent, VQGRAPH still maintains similar performance to GNNs, while GLNN and MLP perform poorly. Furthermore, even when compared with NOSMOG, which leverages adversarial feature augmentation to combat noise and improve robustness, VQGRAPH still outperforms NOSMOG in terms of noise robustness and overall performance across various α settings, due to its superior ability to sufficiently preserve and leverage graph structural information.

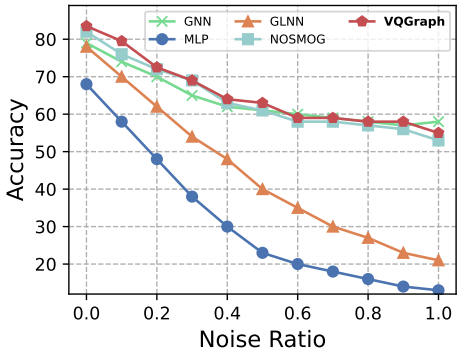

Figure 8: Accuracy vs. Feature Noises.